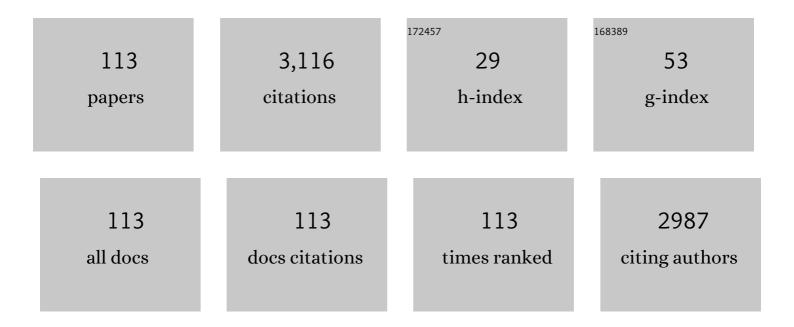
List of Publications by Year in descending order

Source: https://exaly.com/author-pdf/4389476/publications.pdf Version: 2024-02-01



Ηιροςηι Υλο

#	Article	IF	CITATIONS
1	NMR evidence for energy gap opening in thiol-capped platinum nanoparticles. Physical Review B, 2022, 105, .	3.2	1
2	Magnetic Circular Dichroism Study on Dual Plasmonic Au@CuS Core–Shell Nanoparticles: Effects of Shell Thickness and Uniformity. Journal of Physical Chemistry C, 2022, 126, 7933-7940.	3.1	4
3	Unveiling the presence of metallic Co in chemically fabricated Au@CoO core-shell nanoparticles by magnetic circular dichroism (MCD) spectroscopy. Journal of Magnetism and Magnetic Materials, 2022, 560, 169591.	2.3	1
4	Photofunctional organic nanostructures of merocyanine dye fabricated via co-ion-assisted ion association: Morphology transformation from nanospheres to nanofibrils. Chemical Physics, 2022, 562, 111630.	1.9	0
5	On the electronic transitions of α-Fe2O3 hematite nanoparticles with different size and morphology: Analysis by simultaneous deconvolution of UV–vis absorption and MCD spectra. Journal of Magnetism and Magnetic Materials, 2021, 517, 167389.	2.3	13
6	Mixed-diphosphine-protected chiral undecagold clusters Au11(S,S-DIOP)4(rac-/R-/S-BINAP): effect of the handedness of BINAP on their chiroptical responses. Physical Chemistry Chemical Physics, 2021, 23, 16847-16854.	2.8	0
7	Magnetic Circular Dichroism Responses with High Sensitivity and Enhanced Spectral Resolution in Multipolar Plasmonic Modes of Silver Nanoparticles with Dimensions between 90 and 200 nm. Journal of Physical Chemistry Letters, 2021, 12, 9377-9383.	4.6	8
8	Optical and magneto-optical properties of rhodium nanostructures with different morphologies: Insight into the absorption bump in the UV region. Chemical Physics Letters, 2021, 779, 138866.	2.6	1
9	Sensitive detection of small polaron transitions in cesium-doped tungsten bronze CsxWO3 nanostructures using magnetic circular dichroism spectroscopy. Journal of Nanophotonics, 2021, 15, .	1.0	2
10	Fluorescent Organic Lewis-Pair Nanoparticles: Excited-State Intramolecular Proton Transfer Molecule 2-(2â€2-Hydroxyphenyl)benzothiazole Undergoes GSIPT Reactions To Be a Solid-State Nanoemitter. Journal of Physical Chemistry B, 2021, 125, 13937-13945.	2.6	3
11	Organic nanoparticles of anion-based fluorophore 8-anilino-1-naphthalenesulfonate (ANS): Effects of ion-association and post-dilution. Journal of Molecular Structure, 2020, 1200, 127122.	3.6	3
12	Dominant role of iron oxides in magnetic circular dichroism of plasmonic-magnetic Au-Feâ´'O4 heterodimer nanostructures. Journal of Magnetism and Magnetic Materials, 2020, 500, 166385.	2.3	1
13	Chiral–Achiral Ligand Synergy in Enhancing the Chiroptical Activity of Diphosphine-Protected Au ₁₃ Clusters. Journal of Physical Chemistry C, 2020, 124, 25547-25556.	3.1	8
14	Strong chiroptical activity in Au ₂₅ clusters protected by mixed ligands of chiral phosphine and achiral thiolate. Physical Chemistry Chemical Physics, 2020, 22, 15288-15294.	2.8	1
15	Intense Plasmon-Induced Magneto-Optical Activity in Substoichiometric Tungsten Oxide (WO _{3–<i>x</i>}) Nanowires/Nanorods. Journal of Physical Chemistry C, 2020, 124, 15460-15467.	3.1	13
16	Magnetic circular dichroism in plasmonic Ag–Au core–shell nanoparticles: how does the magneto-optical activity tune?. Journal of Nanophotonics, 2020, 14, 1.	1.0	2
17	Magnetic Circular Dichroism of Substoichiometric Molybdenum Oxide (MoO _{3–<i>x</i>}) Nanoarchitectures with Polaronic Defects. Journal of Physical Chemistry C, 2019, 123, 18620-18628.	3.1	11
18	Application of magnetic circular dichroism (MCD) to morphological quality evaluation of silver nanodecahedra. Chemical Physics Letters, 2019, 732, 136637.	2.6	7

#	Article	IF	CITATIONS
19	Chirality in Au ₉ clusters protected by chiral/achiral mixed bidentate phosphine ligands: influence of the metal core and ligand array. Physical Chemistry Chemical Physics, 2019, 21, 14984-14991.	2.8	9
20	Amplified Near-IR Fluorescence in Organic Rhodamine-800 Nanoparticles under the Efficient Control of Aggregation-caused Quenching. Chemistry Letters, 2019, 48, 1339-1342.	1.3	2
21	Size dependence of magneto-optical activity in silver nanoparticles with dimensions between 10 and 60 nm studied by MCD spectroscopy. Physical Chemistry Chemical Physics, 2018, 20, 4269-4276.	2.8	20
22	Water-Soluble Mixed-Phosphine-Protected Gold Clusters: Can a Single Axially Chiral Ligand Lead to Large Chiroptical Responses?. Journal of Physical Chemistry C, 2018, 122, 1299-1308.	3.1	10
23	Organic nanoparticles based on Lewis-pair formation: observation of prototropically controlled dual fluorescence. Photochemical and Photobiological Sciences, 2018, 17, 1376-1385.	2.9	3
24	Magnetic circular dichroism (MCD) in silver nanocubes with different sizes. Chemical Physics Letters, 2018, 706, 607-612.	2.6	8
25	Multipolar Surface Magnetoplasmon Resonances in Triangular Silver Nanoprisms studied by MCD Spectroscopy. Journal of Physical Chemistry C, 2017, 121, 761-768.	3.1	26
26	Organic Ion-Pair Charge-Transfer (IPCT) Nanoparticles: Synthesis and Photoinduced Electrochromism. Langmuir, 2017, 33, 219-227.	3.5	6
27	Water-soluble phosphine-protected Au 9 clusters: Electronic structures and nuclearity conversion via phase transfer. Chemical Physics, 2017, 493, 149-156.	1.9	10
28	Improving the Quality of Electrophoretically-fractionated Chiral Au ₃₈ (SG) ₂₄ Nanoclusters through a Stepwise Phase-transfer Extraction Process: An Absorption and CD Spectroscopic Study. Chemistry Letters, 2017, 46, 104-107.	1.3	2
29	Individual and collective modes of surface magnetoplasmon in thiolate-protected silver nanoparticles studied by MCD spectroscopy. Nanoscale, 2016, 8, 11264-11274.	5.6	33
30	Organic nanoparticles of an extended π-conjugated styryl dye: Modulation of fluorescence peak energy and intensity in the near-infrared (NIR) region. Journal of Photochemistry and Photobiology A: Chemistry, 2016, 330, 140-149.	3.9	5
31	Chiral ligand-protected gold nanoclusters: Considering the optical activity from a viewpoint of ligand dissymmetric field. Progress in Natural Science: Materials International, 2016, 26, 428-439.	4.4	30
32	Magnetic circular dichroism of thiolate-protected plasmonic gold nanoparticles: separating the effects of interband transitions and surface magnetoplasmon resonance. Journal of Nanophotonics, 2016, 10, 046004.	1.0	11
33	Size and morphology effects on the fluorescence properties of π-conjugated poly(p-phenylene) polyelectrolyte nanoparticles synthesized via polyion association. Journal of Materials Chemistry C, 2016, 4, 2945-2953.	5.5	9
34	Water-Soluble Phosphine-Protected Au ₁₁ Clusters: Synthesis, Electronic Structure, and Chiral Phase Transfer in a Synergistic Fashion. Langmuir, 2016, 32, 3284-3293.	3.5	27
35	Enhanced Chiroptical Activity in Glutathione-Protected Bimetallic (AuAg) ₁₈ Nanoclusters with Almost Intact Core–Shell Configuration. Journal of Physical Chemistry C, 2016, 120, 1284-1292.	3.1	24
36	Monolayer-Protected Metal Nanoclusters with Chirality: Synthesis, Size Fractionation, Optical		1

Activity and Asymmetric Transformation. , 2016, , 191-216.

#	Article	IF	CITATIONS
37	Chiral Ligand-Protected Bimetallic Nanoclusters: How does the Metal Core Configuration Influence the Nanocluster's Chiroptical Responses?. Materials Research Society Symposia Proceedings, 2015, 1802, 1-12.	0.1	0
38	Influence of Surface Protonation–Deprotonation Stimuli on the Chiroptical Responses of (<i>R</i>)-/(<i>S</i>)-Mercaptosuccinic Acid-protected Gold Nanoclusters. Chemistry Letters, 2015, 44, 171-173.	1.3	5
39	Fluorescent π-conjugated polymer nanoparticles: A new synthetic approach based on nanoagglomeration via polyion association. Journal of Materials Research, 2015, 30, 10-18.	2.6	2
40	Organic nanoparticles of malachite green with enhanced far-red emission: size-dependence of particle rigidity. Physical Chemistry Chemical Physics, 2015, 17, 11006-11013.	2.8	28
41	Monolayer-Protected Metal Nanoclusters with Chirality: Synthesis, Size Fractionation, Optical Activity and Asymmetric Transformation. , 2015, , 1-22.		0
42	Chiral monolayer-protected Au–Pd bimetallic nanoclusters: Effect of palladium doping on their chiroptical responses. Journal of Colloid and Interface Science, 2014, 419, 1-8.	9.4	15
43	Mechanically inducible fluorescence colour switching in the formation of organic nanoparticles of an ESIPT molecule. Chemical Communications, 2014, 50, 2748-2750.	4.1	23
44	Chiral Monolayer-Protected Bimetallic Au–Ag Nanoclusters: Alloying Effect on Their Electronic Structure and Chiroptical Activity. Journal of Physical Chemistry C, 2014, 118, 15506-15515.	3.1	49
45	Surface magnetoplasmons in silver nanoparticles: Apparent magnetic-field enhancement manifested by simultaneous deconvolution of UV–vis absorption and MCD spectra. Chemical Physics Letters, 2014, 609, 93-97.	2.6	9
46	On the surface structure of 1,3-dithiol-protected gold nanoparticles interpreted by the size effect of IR absorption properties. Colloids and Surfaces A: Physicochemical and Engineering Aspects, 2013, 426, 39-46.	4.7	4
47	Size-dependent spectral linewidth narrowing of H-bands in organic nanoparticles of pentamethine cyanine dye. Journal of Photochemistry and Photobiology A: Chemistry, 2013, 271, 124-129.	3.9	15
48	Emergence of Large Chiroptical Responses by Ligand Exchange Cross-Linking of Monolayer-Protected Gold Clusters with Chiral Dithiol. Langmuir, 2013, 29, 6444-6451.	3.5	12
49	Controlled Formation of Fluorescent Organic Nanoparticles of Carbocyanine Dye via Ion-association Approach. Chemistry Letters, 2012, 41, 1119-1121.	1.3	15
50	On the Electronic Structures of Au ₂₅ (SR) ₁₈ Clusters Studied by Magnetic Circular Dichroism Spectroscopy. Journal of Physical Chemistry Letters, 2012, 3, 1701-1706.	4.6	53
51	Chemical transformation of chiral monolayer-protected gold clusters: observation of ligand size effects on optical and chiroptical responses. Nanoscale, 2012, 4, 955.	5.6	9
52	Boronic Acid-Protected Gold Clusters Capable of Asymmetric Induction: Spectral Deconvolution Analysis of Their Electronic Absorption and Magnetic Circular Dichroism. Langmuir, 2012, 28, 3995-4002.	3.5	12
53	Efficient Excitation-Energy Transfer in Ion-Based Organic Nanoparticles with Versatile Tunability of the Fluorescence Colours. ChemPhysChem, 2012, 13, 2703-2710.	2.1	9
54	Organic Porphyrin Nanoparticles with Induced Optical Activity: Ion-Based Synthesis from Achiral Chromophore and Chiral Counterions. Chemistry of Materials, 2011, 23, 913-922.	6.7	9

#	Article	IF	CITATIONS
55	Highly fluorescent organic nanoparticles of thiacyanine dye: A synergetic effect of intermolecular H-aggregation and restricted intramolecular rotation. RSC Advances, 2011, 1, 834.	3.6	59
56	Organic mediator-induced structural transformation in superlattices of monolayer-protected gold nanoparticles. Journal of Colloid and Interface Science, 2011, 354, 55-60.	9.4	1
57	Synthesis, characterization and optical properties of organic nanoparticles of piroxicam anti-inflammatory drug. Journal of Photochemistry and Photobiology A: Chemistry, 2010, 212, 170-175.	3.9	5
58	Conformational study of chiral penicillamine ligand on optically active silver nanoclusters with IR and VCD spectroscopy. Chemical Physics, 2010, 368, 28-37.	1.9	24
59	Carbon graphite surfaces modified with two-dimensional arrays of N-acetyltripeptide-protected gold nanoparticles. Colloids and Surfaces A: Physicochemical and Engineering Aspects, 2010, 361, 174-179.	4.7	1
60	Prospects for Organic Dye Nanoparticles. Springer Series on Fluorescence, 2010, , 285-304.	0.8	9
61	Induced Optical Activity in Boronic-Acid-Protected Silver Nanoclusters by Complexation with Chiral Fructose. Journal of Physical Chemistry C, 2010, 114, 15909-15915.	3.1	37
62	Gold nanoparticle superlattices self-assembled at a solid/liquid interface. Microelectronic Engineering, 2009, 86, 809-811.	2.4	3
63	Organic Styryl Dye Nanoparticles: Synthesis and Unique Spectroscopic Properties. Langmuir, 2009, 25, 1131-1137.	3.5	43
64	Size Determination of Gold Clusters by Polyacrylamide Gel Electrophoresis in a Large Cluster Region. Journal of Physical Chemistry C, 2009, 113, 14076-14082.	3.1	75
65	Fluorescent Gold Nanoparticle Superlattices. Advanced Materials, 2008, 20, 4719-4723.	21.0	40
66	Effect of organic solvents on J aggregation of pseudoisocyanine dye at mica/water interfaces: Morphological transition from three-dimension to two-dimension. Journal of Colloid and Interface Science, 2008, 318, 116-123.	9.4	10
67	Asymmetric Transformation of Monolayer-Protected Gold Nanoclusters via Chiral Phase Transfer. Journal of Physical Chemistry C, 2008, 112, 16281-16285.	3.1	49
68	Chiral Functionalization of Optically Inactive Monolayer-Protected Silver Nanoclusters by Chiral Ligand-Exchange Reactions. Langmuir, 2008, 24, 2759-2766.	3.5	77
69	Proof of Partial Flattening of Meso Substituents in Tetracationic Porphyrin at a Mica/Solution Interface. Chemistry Letters, 2008, 37, 594-595.	1.3	3
70	Optically Active Gold Nanoclusters. Current Nanoscience, 2008, 4, 92-97.	1.2	56
71	Three-dimensional gold nanoparticle superlattices: Structures and optical absorption characteristics. Journal of Applied Physics, 2007, 101, 114314.	2.5	30
72	Organic Nanoparticles of Cyanine Dye in Aqueous Solution. Bulletin of the Chemical Society of Japan, 2007, 80, 295-302.	3.2	22

#	Article	IF	CITATIONS
73	Chemometric and Microscopic Analyses for the Size Growth of Monolayer-Protected Gold Nanoparticles during Their Superlattice Formation. Langmuir, 2007, 23, 13151-13157.	3.5	4
74	Synthesis and Chiroptical Study ofd/l-Penicillamine-Capped Silver Nanoclusters. Chemistry of Materials, 2007, 19, 2831-2841.	6.7	118
75	Electrolyte-Induced Mesoscopic Aggregation of Thiacarbocyanine Dye in Aqueous Solution:Â Counterion Size Specificity. Journal of Physical Chemistry B, 2007, 111, 7176-7183.	2.6	33
76	Chiroptical Responses of <scp>d</scp> -/ <scp>l</scp> -Penicillamine-Capped Gold Clusters under Perturbations of Temperature Change and Phase Transfer. Journal of Physical Chemistry C, 2007, 111, 14968-14976.	3.1	73
77	Preparation and optical properties of organic nanoparticles of porphyrin without self-aggregation. Journal of Photochemistry and Photobiology A: Chemistry, 2007, 189, 7-14.	3.9	51
78	Self-assembly of acridine orange dye at a mica/solution interface: Formation of nanostripe supramolecular architectures. Journal of Colloid and Interface Science, 2007, 307, 272-279.	9.4	18
79	Selfâ€Assembling of Gold and Silver Nanoparticles at a Hydrophilic/Hydrophobic Interface: A Synthetic Aspect and Superstructure Formation. Synthesis and Reactivity in Inorganic, Metal Organic, and Nano Metal Chemistry, 2006, 36, 237-264.	1.8	20
80	Kinetic Stabilization of Growing Gold Clusters by Passivation with Thiolates. Journal of Physical Chemistry B, 2006, 110, 12218-12221.	2.6	103
81	Fivefold Symmetry in Superlattices of Monolayer-Protected Gold Nanoparticles. Journal of Physical Chemistry B, 2006, 110, 14040-14045.	2.6	33
82	Organic Nanoparticles of Porphyrin without Self-aggregation. Chemistry Letters, 2006, 35, 782-783.	1.3	13
83	Detection of spectral inhomogeneities of mesoscopic thiacyanine J aggregates in solution by the apparent CD spectral measurement. Chemical Physics Letters, 2006, 419, 21-27.	2.6	8
84	Ion-based Organic Nanoparticles: Synthesis, Characterization, and Optical Properties of Pseudoisocyanine Dye Nanoparticles. Chemistry Letters, 2005, 34, 1108-1109.	1.3	16
85	In Situ Detection of Birefringent MesoscopicHandJAggregates of Thiacarbocyanine Dye in Solution. Langmuir, 2005, 21, 1067-1073.	3.5	95
86	Large Optical Activity of Gold Nanocluster Enantiomers Induced by a Pair of Optically Active Penicillamines. Journal of the American Chemical Society, 2005, 127, 15536-15543.	13.7	243
87	Self-Assembly of Si Nanoparticles: Emergence of Two-Dimensional Si Nanoparticle Lattices. Japanese Journal of Applied Physics, 2004, 43, L927-L929.	1.5	9
88	Dynamic morphology of mesoscopic pseudoisocyanine J aggregates on mica induced by humidity treatments. Colloids and Surfaces A: Physicochemical and Engineering Aspects, 2004, 236, 31-37.	4.7	8
89	Large birefringence of single J aggregate nanosheets of thiacyanine dye in solution. Chemical Physics Letters, 2004, 396, 316-322.	2.6	8
90	Interparticle Spacing Control in the Superlattices of Carboxylic Acid-Capped Gold Nanoparticles by Hydrogen-Bonding Mediation. Langmuir, 2004, 20, 10317-10323.	3.5	54

#	Article	IF	CITATIONS
91	Inclusion-Water-Cluster in a Three-Dimensional Superlattice of Gold Nanoparticles. Journal of the American Chemical Society, 2004, 126, 7438-7439.	13.7	47
92	Magic-Numbered AunClusters Protected by Glutathione Monolayers (n= 18, 21, 25, 28, 32, 39):Â Isolation and Spectroscopic Characterization. Journal of the American Chemical Society, 2004, 126, 6518-6519.	13.7	529
93	Collapse and Self-Reconstruction of Mesoscopic Architectures of Supramolecular J Aggregates in Solution: From Strings to Tubular Rods. Letters in Organic Chemistry, 2004, 1, 280-287.	0.5	15
94	Mesodomain separation in amalgamated J aggregate formation of cyanine dyes at a mica/solution interface. Surface Science, 2003, 546, 97-106.	1.9	9
95	Equilibrium growth of three-dimensional gold nanoparticle superlattices. Physica E: Low-Dimensional Systems and Nanostructures, 2003, 17, 521-522.	2.7	29
96	Superstructures of Mesoscopic Monomolecular Sheets of Thiacyanine J Aggregates in Solution. Langmuir, 2003, 19, 8882-8887.	3.5	19
97	Construction of 2D Superlattices of Gold Nanoparticles at an Air/Water Interface Based on Hydrogen-Bonding Networks. Chemistry Letters, 2003, 32, 698-699.	1.3	5
98	Morphology transformation of mesoscopic supramolecular J aggregates in solution. Physical Chemistry Chemical Physics, 2001, 3, 4560-4565.	2.8	31
99	Stepwise Size-Selective Extraction of Carboxylate-Modified Gold Nanoparticles from an Aqueous Suspension into Toluene with Tetraoctylammonium Cations. Chemistry of Materials, 2001, 13, 4692-4697.	6.7	92
100	Particle Crystals of Surface Modified Gold Nanoparticles Grown from Water. Chemistry Letters, 2001, 30, 372-373.	1.3	33
101	Large absorption reduction for mesoscopic thiacyanine J aggregates in solution. Chemical Physics Letters, 2001, 340, 211-216.	2.6	6
102	Phase Transfer of Gold Nanoparticles across a Water/Oil Interface by Stoichiometric Ion-Pair Formation on Particle Surfaces. Bulletin of the Chemical Society of Japan, 2000, 73, 2675-2678.	3.2	41
103	Mesoscopic string structures of thiacyanine J aggregates in solution. Chemical Communications, 2000, , 739-740.	4.1	25
104	Anisotropic Growth of J Aggregates of Pseudoisocyanine Dye at a Mica/Solution Interface Revealed by AFM and Polarization Absorption Measurements. Journal of Physical Chemistry B, 1999, 103, 6909-6912.	2.6	44
105	Spectroscopic and AFM Studies on the Structures of PseudoisocyanineJAggregates at a Mica/Water Interface. Journal of Physical Chemistry B, 1999, 103, 4452-4456.	2.6	60
106	CdS Nanocrystal/Chelate Polymer Hybrid Systems: Controls of Optical and Morphological Properties by Monochromatic Photoirradiation. Polymer Journal, 1999, 31, 1133-1138.	2.7	2
107	Electrolyte Effects on CdS Nanocrystal Formation in Chelate Polymer Particles:Â Optical and Distribution Properties. Langmuir, 1998, 14, 595-601.	3.5	24
108	Surface-InducedJAggregation of Pseudoisocyanine Dye at a Glass/Solution Interface Studied by Total-Internal-Reflection Fluorescence Spectroscopy. Journal of Physical Chemistry B, 1998, 102, 7691-7694.	2.6	24

#	Article	IF	CITATIONS
109	Roles of Interfacial Functions in Analytical Chemistry. Functions of the solid/liquid interface in the J aggregate formation processes Bunseki Kagaku, 1998, 47, 937-943.	0.2	1
110	Microspectroscopic Study on Dye Association at a Single Laser-Trapped Water Droplet/Oil Interface. Langmuir, 1997, 13, 1996-2000.	3.5	12
111	Optical Control of Fusion of Microparticles in Solution and Simultaneous Spectrophotometric Measurements. Analytical Chemistry, 1996, 68, 4304-4307.	6.5	8
112	Micrometer Size Effect on Dye Association in Single Laser-Trapped Water Droplets. The Journal of Physical Chemistry, 1996, 100, 1494-1497.	2.9	25
113	Laser trapping-microspectroscopy of single microparticles Bunseki Kagaku, 1995, 44, 977-987.	0.2	0